Received: 9 May 2018 | Revised: 9 October 2018 | Accepted: 1 November 2018

DOI: 10.1002/hbm.24470

WILEY

RESEARCH ARTICLE

Spontaneous oscillatory markers of cognitive status in two forms of dementia

Priyanka P. Shah-Basak[1,2] | Aneta Kielar[1,2,3] | Tiffany Deschamps[1] | Nicolaas Paul Verhoeff[4,5] | Regina Jokel[1,5,6] | Jed Meltzer[1,2,6,7]

[1]Rotman Research Institute, Baycrest Health Sciences Centre, Toronto, Ontario, Canada

[2]Canadian Partnership for Stroke Recovery, Ottawa, Ontario, Canada

[3]Department of Speech, Language, and Hearing Sciences, University of Arizona, Tucson, Arizona

[4]Department of Psychiatry, University of Toronto, Toronto, Ontario, Canada

[5]Department of Psychiatry, Baycrest Health Sciences, North York, Ontario, Canada

[6]Department of Speech-Language Pathology, University of Toronto, Toronto, Ontario, Canada

[7]Department of Psychology, University of Toronto, Toronto, Ontario, Canada

Correspondence
Priyanka P. Shah-Basak, PhD, Rotman Research Institute, Baycrest Centre, Kimel Family Building, 3560 Bathurst St., Toronto, ON M6A 2E1 Canada.
Email: pshah-basak@research.baycrest.org

Funding information
Canada Research Chairs program; Ontario Brain Institute; Canadian Partnership for Stroke Recovery; Alzheimer's Association

Abstract

Abnormal oscillatory brain activity in dementia may indicate incipient neuronal/synaptic dysfunction, rather than frank structural atrophy. Leveraging a potential link between the degree of abnormal oscillatory activity and cognitive symptom severity, one could localize brain regions in a diseased but pre-atrophic state, which may be more amenable to interventions. In the current study, we evaluated the relationships among cognitive deficits, regional volumetric changes, and resting-state magnetoencephalography abnormalities in patients with mild cognitive impairment (MCI; N = 10; age: 75.9 ± 7.3) or primary progressive aphasia (PPA; N = 12; 69.7 ± 8.0), and compared them to normal aging [young (N = 18; 24.6 ± 3.5), older controls (N = 24; 67.2 ± 9.7]. Whole-brain source-level resting-state estimates of relative oscillatory power in the delta (1–4 Hz), theta (4–7 Hz), alpha (8–12 Hz), and beta (15–30 Hz) bands were combined with gray matter volumes and cognitive scores to examine between-group differences and brain–behavior correlations. Language and executive function (EF) abilities were impaired in patients with PPA, while episodic memory was impaired in MCI. Widespread oscillatory speeding and volumetric shrinkage was associated with normal aging, whereas the trajectory in PPA indicated widespread oscillatory slowing with additional volumetric reductions. Increases in delta and decreases in alpha power uniquely predicted group membership to PPA. Beyond volumetric reductions, more delta predicted poorer memory. In patients with MCI, no consistent group difference among oscillatory measures was found. The contributions of delta/alpha power on memory abilities were larger than volumetric differences. Spontaneous oscillatory abnormalities in association with cognitive symptom severity can serve as a marker of neuronal dysfunction in dementia, providing targets for promising treatments.

KEYWORDS

dementia, magnetoencephalography, mild cognitive impairment, normal aging, primary progressive aphasia, resting-state

1 | INTRODUCTION

Research priorities in mitigating dementia include arresting the neurodegenerative process, providing early diagnosis, and reducing the burden of care. Sensitive biomarkers of dementia severity and treatment effectiveness are critical for these goals. Outcome measures for clinical trials currently focus on conversion from mild cognitive impairment (MCI) to Alzheimer's disease (AD) (Ewers et al., 2012), which requires longitudinal assessments over several years and a large number of participants. For other forms of dementia, such as primary progressive aphasia (PPA), there is currently no consensus on measures that can aid early diagnosis or track disease progression (Tsai & Boxer, 2016). The pace of interventional discovery could be greatly accelerated, if a reliable biomarker of neural dysfunction could be found.

Structural atrophy is one of the most reliable and sensitive measures of dementia (Smith, Andersen, Gold, & Alzheimer's Disease Neuroimaging, 2012). Atrophy reflects a relatively advanced and likely irreversible stage of disease, being a consequence of neuronal cell

death. As dementia progresses from preclinical stages, synaptic damage and loss of neuronal function may comprise an intermediate stage during which cognitive abilities may be compromised in advance of frank atrophy, a stage that is amenable to interventions. Thus, a number of functional neuroimaging approaches have been developed to assess localized neuronal dysfunction, showing profound differences in activation and connectivity patterns accompanying atrophy in the medial temporal lobes in MCI (Sorg et al., 2007; Wang et al., 2006) and the speech and language network in PPA (Hardy et al., 2017; Sonty et al., 2003, 2007).

Electroencephalography (EEG) and magnetoencephalography (MEG) studies have also shown robust alterations in task-based and resting-state signals in patients with dementia (Rossini, Rossi, Babiloni, & Polich, 2007). Specifically, resting-state MEG/EEG studies have found widespread oscillatory/spectral slowing evident as increased delta/theta (low-frequency) power coupled with decreased alpha/beta (high-frequency) power in MCI (Fernandez et al., 2013; Lopez et al., 2014) and in PPA (Ranasinghe et al., 2017). Such slowing is thought to reflect synaptic dysfunction, and prominent shifts toward lower frequencies are associated with steeper decline in cognitive functions (Holschneider & Leuchter, 1995; Leuchter et al., 1993). The findings related to spectral slowing in dementia are of particular importance because they appear in the direction opposite to what is typically seen with normal aging. Healthy elderly adults exhibit decreased low-frequency power and increased high-frequency power (Gomez, Perez-Macias, Poza, Fernandez, & Hornero, 2013; Hashemi et al., 2016), indicating a shift toward faster oscillatory dynamics, contrasting with the patterns reported in dementia.

Recently, our group demonstrated that abnormal neural activity following a stroke can be reliably and sensitively localized to the tissue adjacent to regions of necrosis, using resting-state MEG (rsMEG). Similar to the pathological slowing observed in dementia, perilesional tissue generates low-frequency activity, often in the delta and theta ranges (Chu, Braun, & Meltzer, 2015; Kielar et al., 2016). This tissue exhibits reduced cerebral blood flow, and is likely to have suffered subtle synaptic damage but not cell death as a consequence of stroke. It is unclear, however, what the electrophysiological slowing in MCI and PPA reflects, particularly on the continuum spanning from neuronal synaptic damage, representing a potentially reversible stage of disease, to neuronal atrophy or death.

One way to localize synaptic dysfunction and dissociate it from atrophy is to study the relationships of structural and electrophysiological abnormalities to the severity of cognitive deficits. As such, profound regional volume loss or atrophy may be directly associated with cognitive deficits, and any association of physiological abnormalities with the deficits might simply be a by-product of the volumetric loss. Another possibility is that physiological abnormalities may index incipient neuronal dysfunction rather than atrophy, and the relationship between cognitive deficits and electrophysiological slowing therefore may help localize brain regions in a diseased but pre-atrophic state. To investigate these possibilities, the current study first investigated how spontaneous rsMEG signals in MCI and PPA differ from normal aging, and second, whether the profound alterations in these groups may be localizable to specific brain regions. We combined MRI-based estimates of gray matter (GM) volumes with rsMEG abnormalities to examine how these relate to individual variability in cognitive symptom severity across multiple cognitive domains in MCI and PPA.

2 | METHODS

2.1 | Participants

Sixty-four right-handed native English-speaking participants were assigned to four groups based on age and diagnosis: (1) Young controls (N = 18; mean age: 24.6 ± 3.5 years; 12 males); (2) Older controls (N = 24; 67.2 ± 9.7 years; 18 males); (3) patients with PPA (N = 12; 69.7 ± 8.0 years; 5 males); (4) patients with MCI (N = 10; 75.9 ± 7.3 years; 4 males). See Table 1 for demographic data. Controls were neurologically unimpaired with corrected-to-normal vision, no history of neurological, psychiatric, language, hearing, or learning disorders, and no current neuroleptic or mood-altering medications. PPA patients were diagnosed and classified by a speech language pathologist and/or board certified neurologist based on standard

TABLE 1 Group-wise demographics and clinical variables

Groups	YC	OC	PPA	MCI
N	18	24	12	10
Age (years)	24.6 ± 3.5 (21–34)	67.2 ± 9.7 (45–80)	69.7 ± 8.0 (58–84)	75.9 ± 7.3 (66–90)
Sex	12 M; 6F	18 M; 6F	5 M; 7F	4 M; 6F
Education (years)	17.5 ± 2.5 (14–22)	17.4 ± 2.4 (12–21)	14.7 ± 3.1 (12–20)	14.5 ± 2.2 (12–18)
MoCA (max = 30)		26.5 ± 1.9 (23–30)	19.5 ± 6.3 (7–26)	21.9 ± 3.7 (14–26)
Diagnosis			6 nfvPPA 6 lvPPA	Amnestic
[#]Disease duration (years)			1.3 ± 1.2 (0–4)	

Mean ± standard deviation (*SD*); YC = young controls; OC = older controls; PPA = primary progressive aphasia; nfvPPA = non-fluent variant of PPA; lvPPA = logopenic variant of PPA; MCI = mild cognitive impairment; MoCA = Montreal Cognitive Assessment; max = maximum possible score; M = Male; F = Female; [#]for some PPA patients, we did not have access to their exact dates of diagnosis so we estimated disease duration based on the year of diagnosis; a value of 0 refers to situations where diagnosis and study participation were in the same year.

guidelines (Gorno-Tempini et al., 2011); six patients with effortful, halting speech and/or agrammatic language were classified as having nonfluent variant (nfvPPA), and six patients with impaired word retrieval and phrase/sentence repetition were classified as having logopenic variant (lvPPA). All MCI patients had a consensus diagnosis of amnestic mild cognitive impairment (Petersen, 2004) All patients retained sufficient capacity of language comprehension to provide informed consent and follow task instructions. Exclusion criteria were prior neurological diseases, childhood language disorders, head traumas or brain surgery, severe psychiatric disorders, and unstable or poor health. The study was approved by the Research Ethics Board at Baycrest Health Sciences. Participants provided written informed consent and received financial compensation.

2.2 | Cognitive assessments

Older controls and patients with MCI and PPA completed an extensive neuropsychological battery assessing various domains of cognition, including language, memory, executive function (EF), and visuospatial abilities. Table 2 lists all tests used in this study (Adlam, Patterson, Bozeat, & Hodges, 2010; Benton, Hamsher, Varney, & Spreen, 1983; Cho-Reyes & Thompson, 2012; Delis, Kaplan, & Kramer, 2001; Dunn & Dunn, 1997; Gathercole, Willis, Baddeley, & Emslie, 1994; Kaplan, Goodglass, & Weintraub, 2001; Kay, Lesser, & Coltheart, 1996; Kertesz, 1982; Leach, Kaplan, Rewilak, Richards, & Proulx, 2000; Macwhinney, Fromm, Forbes, & Holland, 2011; Nasreddine et al., 2005; Warrington, 1984).

2.3 | Structural MRI

All participants underwent structural MRI and rsMEG. MRI was carried out on a 3-Tesla scanner (Siemens TIM Trio). For MEG source localization and Voxel Based Morphometry (VBM) analyses, we used a T1-weighted MPRAGE image (1 mm isotropic voxels, TR = 2,000 ms, TE = 2.63 ms, FOV = 256 × 256 mm^2, 160 axial slices, scan time 6 m, 26 s). MR-visible markers were placed at the fiducial points for accurate co-registration with MEG, aided by digital photographs. T1-images were skull stripped in AFNI (http://afni.nimh.nih.gov/).

2.4 | Voxel-based morphometry

Voxel-based Morphometry (VBM) implemented in SPM12 (Wellcome Department of Cognitive Neurology, London, UK), was used to derive segmented, spatially normalized, bias corrected, and smoothed GM maps for participants in all groups (Ashburner & Friston, 2005). Before processing, T1 images were evaluated for quality and manually repositioned to set the anterior commissure as the origin to ensure consistent starting estimates for the unified segmentation routine. To increase the accuracy of inter-participant alignment, nonlinear deformation parameters were calculated with the high dimensional diffeomorphic anatomical registration through exponentiated lie (DARTEL) algorithm and the predefined templates within the SPM DARTEL

TABLE 2 Neuropsychological battery completed by all older controls, PPA, and MCI patients

Domain	Tests
General cognitive status	Montreal cognitive assessment (MoCA; Nasreddine et al., 2005)
Aphasia severity	Western aphasia battery-revised bedside record form (WAB; Kertesz, 1982) for classification of aphasia type
	Selected subtests of reading, spelling and repetition from psycholinguistic assessments of language processing in aphasia (PALPA; Kay et al., 1996) to supplement WAB
Verbal fluency	Letter fluency tests (letters FAS) from Delis–Kaplan executive function system (D-KEFS; Delis et al., 2001)
Confrontational naming	60-item Boston naming test (BNT; Kaplan et al., 2001)
Comprehension and production of sentences varying in syntactic complexity	Two subtests of the northwestern assessment of verbs and sentences (NAVS; Cho-Reyes & Thompson, 2012)—Sentence comprehension test (SCT) sentence production priming test (SPPT)
Comprehension and production of isolated verbs	Subtests of NAVS including verb naming and verb comprehension tests (VNT, VCT)
Verb production in a sentence context	A subtest of NAVS, argument structure production test (ASPT)
Repetition	Sentence repetition (SR) tests from the AphasiaBank repetition test (Macwhinney et al., 2011) including stimulus items with increasing length (SR-A) and those with and without errors (SR-B)
Receptive lexical semantics and vocabulary knowledge	Peabody picture vocabulary test, fourth edition (PPVT; Dunn & Dunn, 1997)
Semantic knowledge independent of expressive verbal abilities	Camel and cactus test (CCT; Adlam et al., 2010)
Phonological working memory	Children's test of nonword repetition (CNRep; Gathercole et al., 1994)
Episodic memory	Word lists (WL; immediate and delayed free and cued recall, and recognition) from the Kaplan Baycrest neurocognitive assessment (KBNA; Leach et al., 2000), and the logical memory (LM) subtest from Wechsler memory scale -IV (WMS-IV; LM - immediate, delayed recall, and recognition)
Non-verbal episodic memory	Facial recognition test (Warrington, 1984)
Executive function	Digit span forward and backward from Wechsler adult intelligence scale (WAIS-IV) battery and the trails making test (TMT-A and TMT-B) from the D-KEFS battery
Visuospatial abilities	Complex figure (CF; immediate: Copy and recall, delayed: Recall and recognition), symbol cancelation both from KBNA, and a short form of Benton's judgment of line orientation test (JLO; Benton et al., 1983).

toolbox (Ashburner, 2007). For each participant, flow fields were calculated during template creation that contained the nonlinear deformation information on the native image transformation to the template. These flow fields were applied to each participant's image. Next, the final template was registered to MNI space using an affine transform and this transformation was incorporated into the warping process, so that the individual spatially normalized scans could be brought into the common MNI space. During this final normalization step, the gray and white matter probability maps were scaled by their Jacobian determinants and smoothed using a 10 mm FWHM isotopic Gaussian kernel. The GM volumes were downsampled to match the resolution of the MEG power maps for voxel-wise GM and MEG comparisons between-groups, and comparisons within-group with cognitive measures.

2.5 | MEG acquisition and analysis

MEG signals were recorded with a 151-channel whole-head system with axial gradiometers (VSMMedTech, Coquitlam, Canada). MEG was recorded continuously at a sampling rate of 625 Hz, and acquired with online synthetic 3rd-order gradient noise reduction. Head position with respect to the MEG helmet was monitored using three coils placed at fiducial landmarks of the head (nasion, left, and right preauricular points). Head positions were measured before and after the resting-state run, and the two positions were averaged. The multisphere head models for MEG analysis (Huang, Mosher, & Leahy, 1999) were constructed using the T1-weighted MRI. The resting state MEG recording was divided into arbitrary 2.5-s epochs for analysis and averaging. MEG source analysis was conducted on a whole-brain grid of locations spaced 10 mm apart using Synthetic Aperture Magnetometry (SAM) (Vrba & Robinson, 2001), as implemented in CTF software (CTF; Port Coquitlam, British Columbia, Canada), supplemented with in-house MATLAB scripts. SAM is a scalar beamformer, in which a nonlinear optimization technique is used to select one direction of current flow at each voxel to maximize dipole power. In short, SAM provides a series of sensor weights for each voxel; the weights are computed so as to pass signal from a dipole located in the target voxel, while minimizing signal power from all other locations. We computed weights on a whole-brain grid of locations spaced 10 mm apart. These weights were then multiplied with the original sensor time series data to yield a new, spatially filtered, time series signal at each voxel (10 mm^3). Normalized weights were used to render virtual signals in dimensionless units of signal-to-noise ratio, with noise power estimated as the lowest singular value of the sensor covariance matrix (Vrba & Robinson, 2001). Signals were filtered at 0–100 Hz prior to beamforming. Raw MEG sensor signals were screened for motion (e.g., coughs, sneezes, yawns, head movements) and environmental artifacts, and epochs containing obvious signal disruptions or drifts were rejected (<1% of all epochs). The SAM beamformer procedure effectively attenuates physiological artifacts such as those from muscle activity and eye movements or blinks (Cheyne, Bostan, Gaetz, & Pang, 2007; Vrba, 2002). Therefore, the epochs containing these artifacts were not rejected manually.

Power spectral densities of the voxel-wise virtual signals were computed using the multitaper method in MATLAB (Thomson, 1982). The time half bandwidth [NW] was set to 3, which resulted in 5 (2*(NW)-1) discrete prolate spheroidal or Slepian sequences for multitaper computations. A frequency resolution of 0.3052 Hz was achieved with FFT length of 1,024 and sampling frequency of 625 Hz. Relative power was computed for each canonical frequency band—delta (1–4 Hz), theta (4–7 Hz), alpha (8–12 Hz), and beta (15–30 Hz)—as a ratio of the sum of power within a frequency band and the sum of total power from 1–80 Hz.

2.6 | Statistical analysis

2.6.1 | Derivation of cognitive factor scores

For dimensionality reduction of the large set of individual neuropsychological test scores, we performed Principal Components Analysis (PCA) with Varimax rotation (rPCA) (Kaiser, 1958). rPCA was expected to reveal an optimal linear combination of test scores for separating cognitive abilities, instead of simply averaging the test scores within each domain. All test-scores were z-scored prior to PCA. PCA and Varimax rotation were implemented using the psych package in RStudio (version 1.1.383). One-way ANOVAs were conducted on factor scores for comparisons across groups; the scores were rank-transformed to ensure the assumptions of normality and homogeneity of variance were met. Significant main effects of group were further evaluated with post-hoc pairwise *t*-tests corrected for multiple comparisons using Holm's method.

2.6.2 | Between-group, whole-brain comparisons of MEG spectral power and GM volumes

Three separate task Partial Least Squares (PLS) (McIntosh, Bookstein, Haxby, & Grady, 1996) analyses were conducted to compare relative spectral power estimates in each of the frequency bands and the GM volume estimates between: (1) older and younger controls, (2) PPA and age-matched controls, and (3) MCI and age-matched controls. As opposed to univariate statistical approaches, multivariate methods such as PLS do not necessitate corrections for multiple comparisons because the statistical inference testing is done at the level of full multivariate pattern rather than at the level of individual voxels. Additionally, PLS handles highly correlated dependent variables in the dataset (McIntosh & Lobaugh, 2004). For these two reasons, we adopted the Task PLS analysis framework for our group comparisons.

For each of the PLS group comparisons, the input data matrices had *n* rows of participants, nested within groups (*design variables*) and *v* columns of relative power values for each frequency band and GM volumes (*brain* variables), nested within voxels. PLS, unlike PCA, estimates the maximal covariance between two different types of data blocks (Misic et al., 2016). PLS in our case was expected to generate *saliences* representing the brain variables, consisting of voxelwise relative power estimates and GM volumes (brain saliences), and the experimental design variables, describing the groups (design saliences). The output of PLS, referred to as latent variables (LV), is a composite of singular values, which describe the maximal covariance between the brain and the design variables, and two singular vectors with brain and design saliences. Saliences are the weights, likened to factor loadings in PCA, for each input data block. Linear combination of brain saliences with the input data matrix provides brain scores per

participants, which are likened to factor scores in PCA. For our group comparisons, two LVs per comparison were produced.

Statistical inference of LVs was determined by permutation tests with 1,000 iterations with a threshold of $p < .05$. These tests indicated which LVs were significant as an entire multivariate pattern. To identify brain voxels making a significant contribution to the LV pattern, we employed bootstrapping with 500 resamples to compute the standard errors (SE) of brain saliences. Bootstrap ratios (BSR) were computed as a ratio of the brain saliences and the bootstrap SEs, which provided an estimate of the reliability of contributions of brain saliences. For significant LVs, BSR maps were interpreted at thresholds of ± 4.0 for highly stable results (Misic et al., 2016).

2.6.3 | Whole-brain comparisons with cognitive factor scores

Behavioral PLS analyses were performed within each patient group for brain–behavior correlations between cognitive factor scores and brain variables. Separate PLS analyses were conducted for correlations with each cognitive factor. The methods for determining statistical significance and reliability of brain saliences were the same as the task PLS procedures. The Rotman PLS toolbox in MATLAB (McIntosh et al., 1996) was used for both task and behavioral PLS analyses.

2.6.4 | Regions-of-interest analyses

Although the whole-brain PLS identifies significant relationships between oscillatory power, GM volume, group status, and cognition, the possibility exists that such relationships could be confounded or mediated by additional factors not included in the model. Because it is not feasible to interpret coefficients of complicated multiple regression models mapped across the whole brain, we identified brain areas exhibiting the strongest effects in the whole-brain PLS analyses for followup regions-of-interest (ROI) analyses, which involved modeling using either a logistic or a multiple linear regression model. There is always a concern for circularity in using data-driven ROI selection (Kriegeskorte, Simmons, Bellgowan, & Baker, 2009), in that characterizing effect sizes on an ROI selected for exhibiting the very effect in question will inflate the observed effect size. However, in the present case, the goals of the ROI analysis were (1) to rule out the contributions of nuisance factors (e.g., age, disease duration), and (2) to test whether the oscillatory slowing present in dementia makes an independent contribution to variance in cognitive status beyond that accounted for by atrophy alone. By focusing the ROI analyses on areas showing strong effects of GM volume and oscillatory changes, we maximize our ability to distinguish mediating and moderating relationships among these variables.

The dependent variable for the logistic regression model was a binomial grouping variable: age-matched controls versus one of the patient groups. In multiple regression analysis, the dependent variable was one of the cognitive factor scores. The independent variables were relative spectral power, GM volumes, and age, sex, and/or disease duration as covariates in both these analyses. If the spectral power and GM volumes were not correlated in a given ROI, we conducted likelihood ratio tests to compare models with and without GM volumes along with spectral power to examine their relative contributions in improving the model fit. In ROIs where they were significantly correlated, we inspected the regression coefficients associated with each of these variables in individual analyses, and followed by a combined analysis to assess their unique contributions, after controlling for the other variable. In these cases, mediation analysis (MacKinnon, Fairchild, & Fritz, 2007) was also conducted to further evaluate the indirect effects of GM volumes.

3 | RESULTS

3.1 | Cognitive testing

MoCA scores differed across older healthy controls (26.5 ± 1.9), MCI (21.9 ± 3.7), and PPA (19.5 ± 6.3) groups ($F[2,43] = 14.1$, $p < .001$), with significant differences between controls and MCI ($p = .006$) and controls and PPA ($p < .001$), but not between MCI and PPA ($p = .16$).

PCA on the cognitive battery including 27 test scores (Table 2) resulted in 26 factors. The eigenvalues of the first four factors were 11.6, 4.1, 2.2, and 1.7, respectively, and explained 67% of the total variance. This four-factor solution was submitted to Varimax rotation, resulting in four Rotated Components (RC). The set of rotated factors and loadings greater than 0.35 were examined for their mapping onto the cognitive domains of interest (Figure 1a). Additionally, BSRs were computed for each of the RCs as a ratio of the original loadings and corresponding bootstrap SE which was estimated from 2,000 bootstrap samples. The mapping of RCs onto cognitive domains was interpreted based on loadings that survived the threshold of BSR > 2.0.

Tests that loaded highly onto the first factor (RC1) had clear verbal or language elements, identifying it as a language factor. Tests of sentence comprehension, production and verb naming, and confrontational naming, sentence repetition, and nonword repetition tests all had loadings >0.5 and BSR >2.0. Additionally, logical memory (LM) tests, which required verbal recall or recognition of passages, also had high loadings with immediate recall having the highest loading among the LM test scores.

The second factor (RC2) appeared to map onto episodic memory function. Tests involving immediate and delayed recall and recognition of both verbal (LM, word list) and non-verbal (complex figure, face recognition) items weighted highly on this factor.

The third factor (RC3) appeared to map onto EF and short-term memory. Tests such as TMT -B and letter fluency, and also tests including digit span (both backward and forward), and the immediate (but not delayed) recall of WL and LM weighted highly on this factor.

The fourth factor (RC4) was the most difficult to interpret, as the loadings were high across several tests and factors but only three met the BSR threshold of 2.0. Based on the pattern of loadings, it may involve conceptual semantics. RC4 was weighted by the CCT, reflecting conceptual semantic knowledge and by the NAVS subtests involving verb and sentence comprehension, which may involve semantic processing besides EF.

A significant main effect of group across the older controls, PPA and MCI groups (Figure 1b) was found for RC1-language ($F[2,45] = 6.81$, $p = .003$; Figure 1b), RC2-memory ($F[2,45] = 22.5$, $p < .001$; Figure 1c), and RC3-EF ($F[2,45] = 4.82$, $p = .013$; Figure 1d) but not for RC4 scores ($p = .57$). Post-hoc t-tests indicated that the mean RC1-language scores were significantly lower in PPA ($p = .002$), but not in MCI, the mean RC2-memory scores were significantly lower in MCI ($p < .001$) but not in PPA ($p = .30$), and the mean RC3-EF scores were lower in PPA

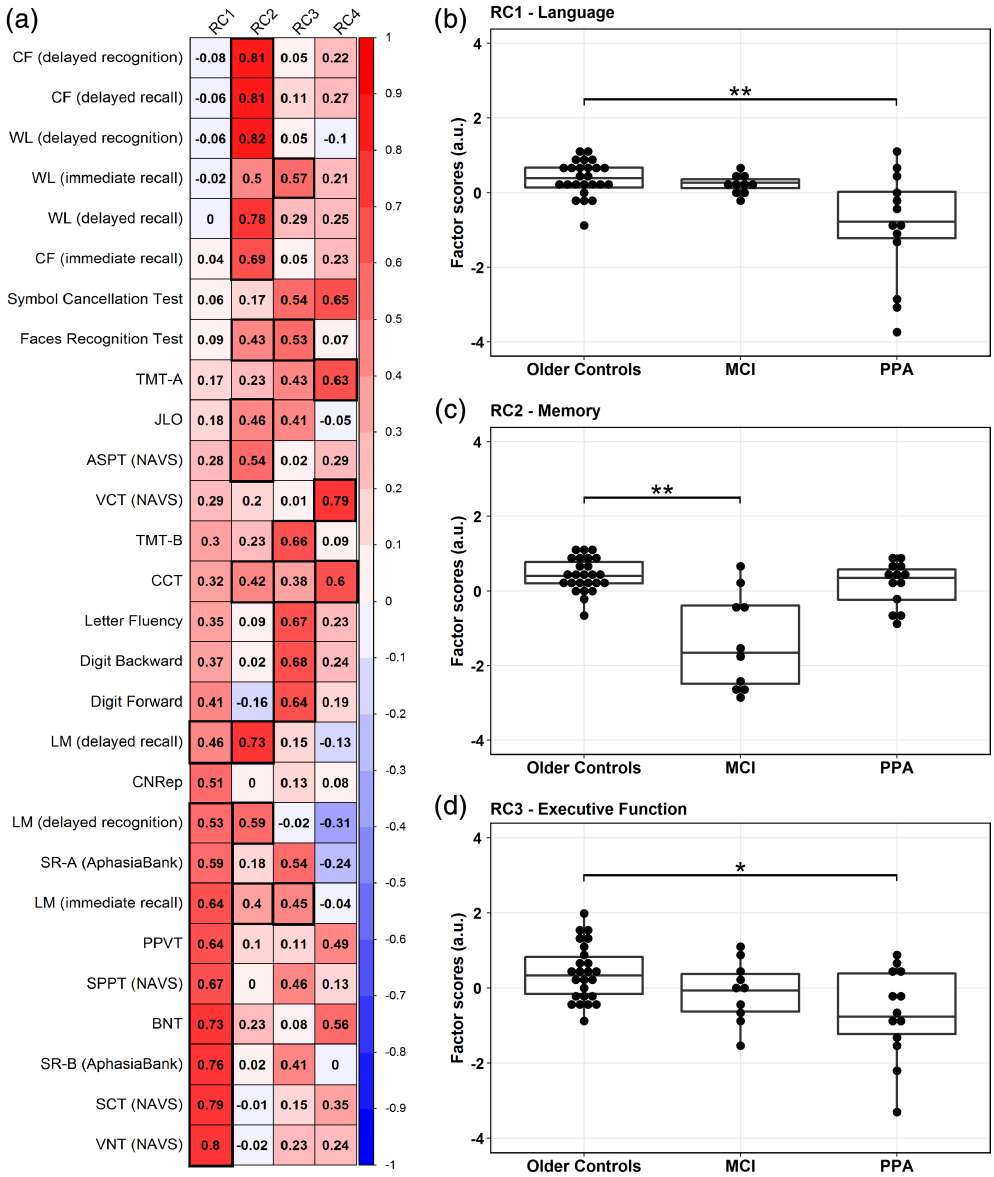

FIGURE 1 Results from the rotated principal component analysis (rPCA) on cognitive test scores. (a) Factor loadings representing the positive (in red) and the negative (in blue) correlations between cognitive test scores and four factors or rotated components (RC1-4) derived from rPCA. Factor loadings with bootstrap ratios greater than 2.0 are highlighted by thick black lines. The first three RCs loaded highly onto test scores of language (RC1), memory (RC2) and executive function (RC3) abilities, respectively. RC1-language (b) and RC3-executive function (d) scores significantly differed between older controls and PPA but not MCI, whereas MCI differed from older controls on RC2-memory (c) scores; horizontal lines within the boxplots in b–d represent the median, the bars represent the interquartile range, and the superimposed dots represent individual data points. a.u. = arbitrary units; *significance at $p < .05$; **significance at $p < .001$ [Color figure can be viewed at wileyonlinelibrary.com]

($p = .012$) but not in MCI, all compared with the older controls. Mean RC2-memory scores were significantly lower in MCI compared with PPA patients ($p = .01$), while there was a trend toward lower RC1-language scores in PPA compared with MCI patients ($p = .08$).

3.2 | MEG/MRI effects of age in controls: Older versus younger group comparisons

The first LV (LV1) was significant ($p < .001$), indicating a main effect of group (Figure 2). The mean-centered brain score average was ±7.1 (95% CI: 6.5–8.5). Compared with younger controls, older controls exhibited less relative power in the delta and theta bands, and higher power in the alpha and beta bands. Decreases in delta and theta involved the superior (SFG) and medial frontal gyri (MeFG), superior/middle temporal, and parietal regions, whereas decreases in delta but not in theta were found in the parahippocampal gyrus (PHG) and thalamus. Alpha increases involved the middle (MTG) and superior temporal gyri (STG), with more left than right involvement, whereas beta increases were present bilaterally primarily in the SFG and MeFG. GM volumes were also significantly decreased as expected in older controls across a large number of areas, but the occipital, inferior temporal, and superior parietal areas appeared to be less affected. We also tested for an association with age within the older group alone. There was no significant effect within the older group alone, but LV1 had a

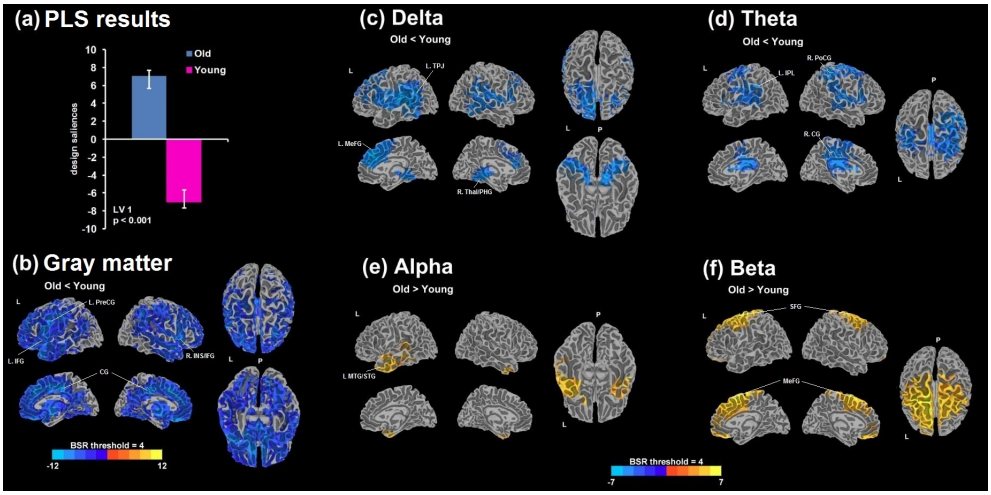

FIGURE 2 (a) Design saliences from a significant latent variable 1 (LV1; $p < .001$) obtained from the partial least squares (PLS) analysis comparing *young and older controls*. Bootstrap ratio (BSR) maps thresholded at ±4.0 are shown for the differences in gray matter (GM) volumes (b) and the relative MEG power estimates of delta (c), theta (d), alpha (e), and beta (e); the overlay maps were smoothed using the linear resampling mode in AFNI and the 3D cortical surface render with BSR were generated using the AFNI-SUMA suite. Positive values of BSR (red-yellow) demonstrate a positive association with the design saliences, that is, older > younger, and negative values of BSR (blue) demonstrate a negative association, that is, older < younger. L = left; R = right; P = posterior; PreCG = precentral gyrus; IFG = inferior frontal gyrus; CG = cingulate gyrus; INS = insula; TPJ = temporoparietal junction; MeFG = medial frontal gyrus; Thal = thalamus; PHG = parahippocampal gyrus; IPL = inferior parietal lobe; PoCG = postcentral gyrus; MTG = middle temporal gyrus; STG = superior temporal gyrus; SFG = superior frontal gyrus [Color figure can be viewed at wileyonlinelibrary.com]

trend ($p = .099$) in the opposite direction of the older versus younger difference—increasing age was associated with more delta and less beta, suggesting a U-shaped trajectory of spectral content throughout the aging process.

3.3 | PPA and MCI differ from the age-matched controls

For the comparison of the PPA group versus the age-matched controls, LV1 was significant ($p < .001$), depicting the main effect of group (Figure 3). The mean-centered brain score average was ±6.6 (95% CI: 5.6–9.1). Compared with the controls, PPA patients exhibited more delta and theta power, less alpha and beta power, and smaller GM volumes. Increases in delta power were prominent in the right thalamus, left anterior cingulate gyrus (ACC), right SFG, right PHG, and right middle frontal gyrus (MFG) areas. Reductions in alpha were mainly localized to the left language processing areas, including the left fusiform gyrus (FFG), and the inferior frontal gyrus (IFG) and the MTG, overlapping with areas exhibiting GM volume reductions. Additionally, alpha reductions extended to the inferior temporal gyrus (ITG) and

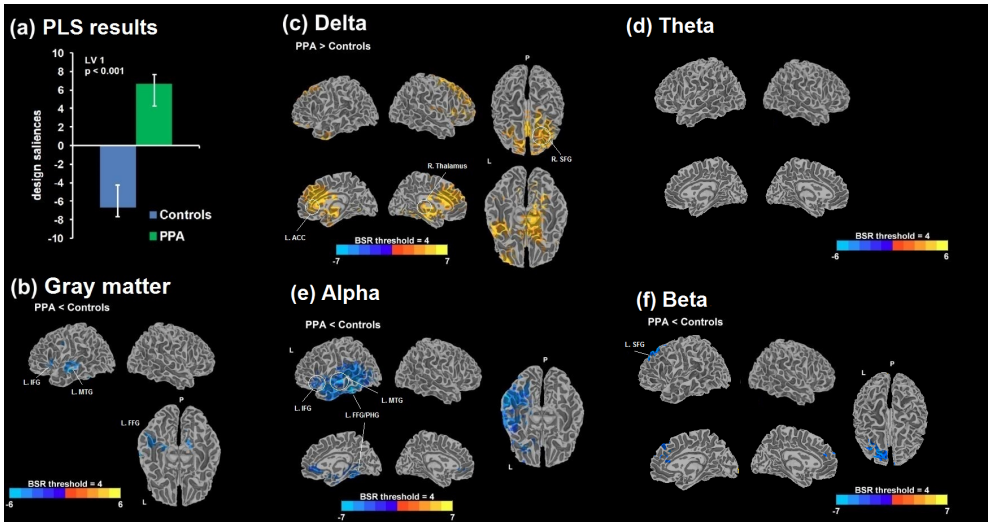

FIGURE 3 (a) Design saliences from a significant latent variable 1 (LV1; $p < .001$) obtained from the PLS analysis comparing *PPA and age-matched* controls. Bootstrap ratio (BSR) maps thresholded at ±4.0 are shown for the differences in GM volumes (b) and the relative MEG power estimates of delta (c), theta (d), alpha (e), and beta (e); positive values of BSR (red/yellow) demonstrate a positive association with the design saliences, that is, PPA > controls, and negative values of BSR (blue) demonstrate a negative association, that is, PPA < controls. PLS = partial least squares; L = left; R = right; P = posterior; IFG = inferior frontal gyrus; MTG = middle temporal gyrus; FFG = fusiform gyrus; PHG = parahippocampal gyrus; ACC = anterior cingulate cortex; SFG = superior frontal gyrus [Color figure can be viewed at wileyonlinelibrary.com]

medially into PHG and ACC. Power differences in beta were found in left SFG, extending into the ACC. None of the differences in theta survived the BSR threshold of 4.0. Overall, these results suggested a dissociation in the direction of spectral changes, characterizing PPA patients differently from the normally aging controls.

For the comparison of MCI vs. age-matched controls, LV1 was not significant (p = .15). Given that the magnitude of changes in MCI may be smaller compared with PPA, we conducted separate analyses with only the GM volumes or the spectral power estimates. LV1 tended toward significance (p = .067) with GM volumes, while LVs for power estimates were not significant. GM volume in the basal forebrain and limbic structures, involving bilateral PHG and surrounding brain regions, tended to be smaller. Other regions such as the left lingual/occipital, the left MTG and the right cuneus also appeared to be smaller in MCI (Supporting Information Figure S1). These results represent a tendency for volume loss in MCI in regions typically associated with episodic memory functions, whereas no measurable differences were found in power estimates.

3.4 | Significant correlations with cognition in PPA and MCI

Within the PPA group, LV1 was significant for spectral power and GM volume correlations with RC2-memory (p = .011; Figure 4) as well as with RC3-EF (p = .027; Figure 5) factor scores, while the LVs for RC1-language and RC4 scores were not significant. The correlation of RC2-memory with LV1 scores was 0.83 (95% CI: 0.81–0.96), and that for RC3-EF was 0.79 (95% CI: 0.77–0.94).

RC2-memory was negatively correlated with delta and theta, and positively correlated with beta, indicating that greater low-frequency power and lesser high-frequency power were both associated with poorer memory performance in PPA. None survived the BSR threshold of 4 for the alpha band. The areas exhibiting negative correlations in delta included bilateral MeFG, ACC, and IFG in addition to the left lingual, left precentral gyrus (PreCG), right MTG, left STG, right thalamus, and right parietal regions. Correlations with theta and beta were particularly interesting as they formed a large cluster, encompassing the left temporoparietal junction (TPJ). Negative theta correlations extended to other areas including the left precuneus (PreCun) and cuneus, left PHG, and FFG. Positive correlations with beta were found in the left insula, right posterior cingulate gyrus (PCC), left PreCun and right cuneus, left FFG, right PHG, and postcentral gyrus (PostCG). RC2 scores and GM volumes were positively correlated, indicating that more preserved GM volume predicts better memory performance. The areas involved were widespread, including the left PostCG, bilateral PreCun, right IFG, left MTG, right FFG, right angular gyrus (AG), left MFG, left STG, right MTG, and bilateral cingulate gyri.

A negative correlation of RC3-EF scores was found with theta and alpha, and a positive correlation with beta in PPA. Lesser theta in bilateral SFG extending medially into the right PCC and cuneus/calcarine gyrus and cingulate gyrus, and lesser alpha in bilateral SFG extending into MFG, IFG and medial frontal gyrus, were both linked with higher scores. More beta in bilateral paracentral/PreCun, lingual gyri and cuneus, left insula, left SPL, and left FFG were also linked with higher scores. Finally, GM volumes and RC3-EF scores were positively correlated in the bilateral caudate and precuneus, indicating that more preserved GM volume in these areas was associated with better EF performance.

Within the MCI group, LV1 was significant for RC2-memory scores (p = .014), with a correlation of 0.88 (95% CI: 0.87–0.98). None of the LVs for other cognitive factor scores were significant. A negative correlation with delta and theta, and a positive correlation with

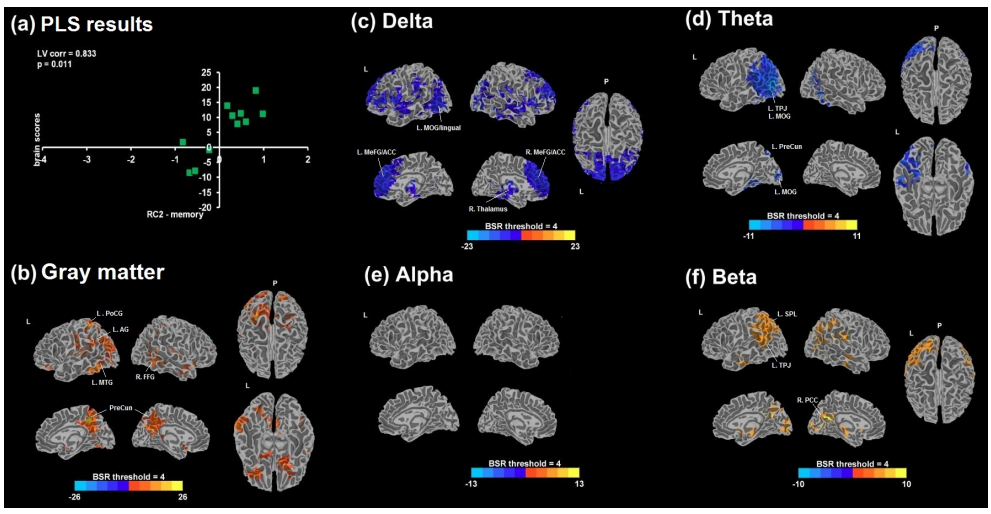

FIGURE 4 (a) Scatter plot between design (RC2-memory factor scores) and brain scores from a significant latent variable 1 (LV1; p = .011) obtained from the behavioral PLS analysis in *PPA with RC2 scores* are displayed. Bootstrap ratio (BSR) maps thresholded at ±4.0 are shown for the correlation with GM volumes (b) and the relative MEG power estimates of delta (c), theta (d), alpha (e), and beta (e); positive BSR values (red/yellow) demonstrate a positive correlation, and negative BSR values (blue) demonstrate a negative correlation. PLS = partial least squares; L = left; R = right; P = posterior; corr = correlation; PoCG = postcentral gyrus; AG = angular gyrus; MTG = middle temporal gyrus; PreCu*n* = precuneus; FFG = fusiform gyrus; MOG = middle occipital gyrus; MeFG = medial frontal gyrus; ACC = anterior cingulate cortex; TPJ = temporoparietal junction; SPL = superior parietal lobe; PCC = posterior cingulate cortex [Color figure can be viewed at wileyonlinelibrary.com]

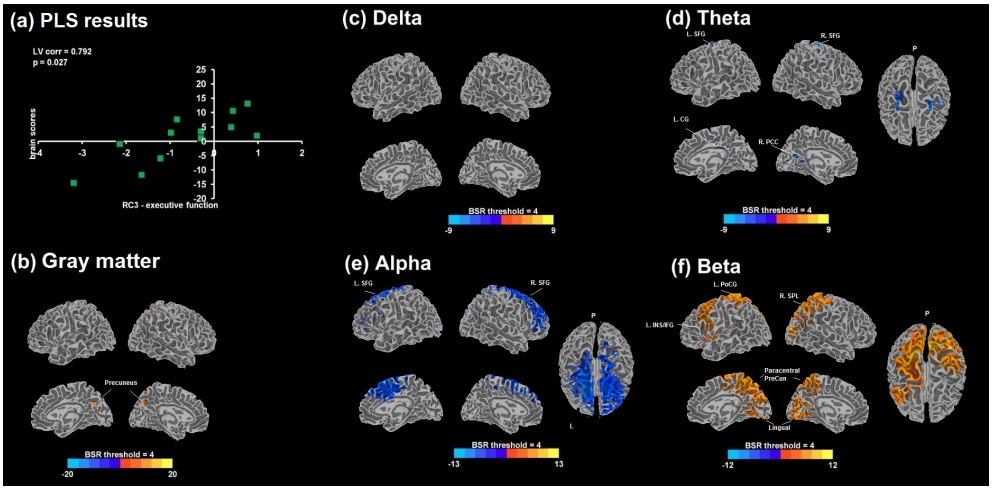

FIGURE 5 (a) Scatter plot between design (RC3-executive function factor scores) and brain scores from a significant latent variable 1 (LV1; p = .027) obtained from the behavioral PLS analysis in *PPA with RC3 scores* are displayed. Bootstrap ratio (BSR) maps thresholded at ±4.0 are shown for the correlation with GM volumes (b) and the relative MEG power estimates of delta (c), theta (d), alpha (e), and beta (e); positive BSR values (red/yellow) demonstrate a positive correlation, and negative BSR values (blue) demonstrate a negative correlation. PLS = partial least squares; L = left; R = right; P = posterior; corr = correlation; PCC = posterior cingulate cortex; CG = cingulate gyrus; PreCu*n* = precuneus; SPL = superior parietal lobe; MTG = middle temporal gyrus; PoCG = postcentral gyrus; SFG = superior frontal gyrus; INS = insula; IFG = inferior frontal gyrus [Color figure can be viewed at wileyonlinelibrary.com]

alpha power were found (Figure 6). Lesser delta in the bilateral SPL and IPL, PreCun, PCC, insula, right PostCG, left PHG, left cuneus, and left middle occipital gyrus (MOG) was associated with higher scores. More alpha in the left cuneus, lingual, PreCG, SFG and MeFG, bilateral STG, and left PCC was associated with higher scores. Negative theta correlations were found in the left PreCun, left paracentral lobule, left middle cingulate gyrus, and bilateral MeFG. None of the correlations with beta power survived the BSR threshold of 4.0. RC2-memory and GM volumes were positively correlated, indicating that more preserved volumes in the bilateral PostCG, IPL, PHG, IFG, left lingual gyrus, left PCC, and bilateral MTG were associated with better memory performance in MCI.

3.5 | ROI analyses revealed unique contributions of spectral abnormalities

3.5.1 | PPA versus age-matched controls

The group differences between PPA and age-matched controls were further scrutinized in an ROI-based logistic regression analysis. ROIs were selected based on the most stable whole brain results (Supporting

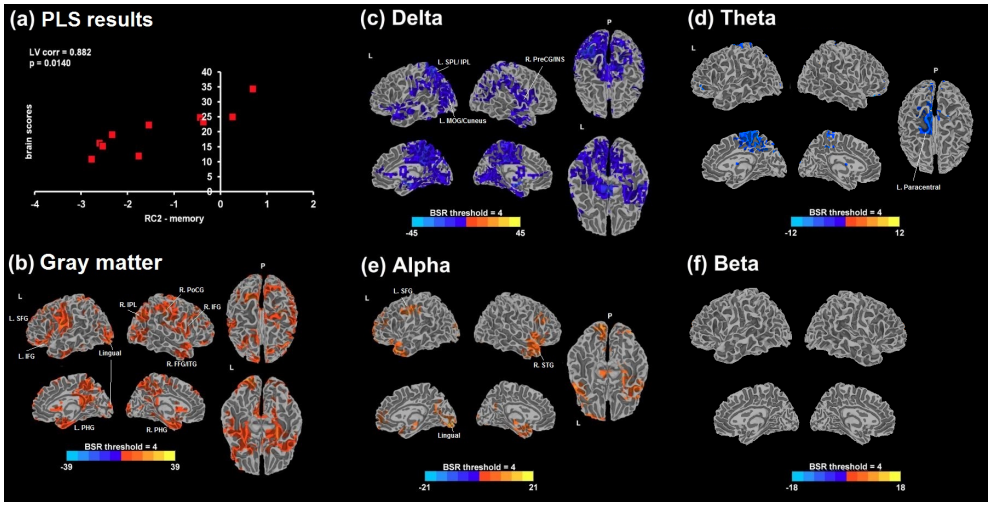

FIGURE 6 (a) Scatter plot between design (RC2-memory factor scores) and brain scores from a significant latent variable 1 (LV1; p = .014) obtained from the behavioral PLS analysis in *MCI with RC2 scores* are displayed. Bootstrap ratio (BSR) maps thresholded at ±4.0 are shown for the correlation with GM volumes (b) and the relative MEG power estimates of delta (c), theta (d), alpha (e), and beta (e); positive BSR values (red/yellow) demonstrate a positive correlation, and negative BSR values (blue) demonstrate a negative correlation. PLS = partial least squares; L = left; R = right; P = posterior; corr = correlation; SFG = superior frontal gyrus; IFG = inferior frontal gyrus; PHG = parahippocampal gyrus; IPL = inferior parietal lobe; PoCG = postcentral gyrus; FFG = fusiform gyrus; ITG = inferior temporal gyrus; SPL = superior parietal lobe; MOG = middle occipital gyrus; PreCG = precentral gyrus; INS = insula; STG = superior temporal gyrus [Color figure can be viewed at wileyonlinelibrary.com]

Information Table S1). Group membership to PPA (vs. controls) was significantly predicted by delta in the right thalamus (b = 48.7, p = .043) and in the right SFG (b = 47.1, p = .021), and there was a trend for the left ACC (b = 27.2, p = .081), after controlling for sex and GM volumes (Supporting Information Table S1). The effects of alpha in the left FFG/PHG (b = −26.5, p = .038) remained significant after controlling for the covariates, whereas for the other two ROIs, there was a trend (left MTG: p = .067; left IFG: p = .076). The effects of beta in left SFG (b = −25.7, p = .020) remained significant after controlling for the covariates. The relationship with theta was not examined as none of the areas survived the BSR threshold in the whole-brain analysis. Together, these results suggest that delta and alpha power uniquely contribute to the group differences, beyond the putative effects of GM volumes and demographic variables.

3.5.2 | PPA RC2-memory

Adding GM volumes did not improve the model fit in the bilateral MeFG and right thalamus ROIs. The effects of delta on RC2-memory scores were significant (bilateral MeFG: b = −7.0, p = .017; left MOG: b = −7.6, p = .010; right thalamus: b = −12.4, p = .008) after controlling for age, GM volumes, and disease duration in all three ROIs (Supporting Information Table S2). Disease duration and memory performance appeared to be related but the contribution of delta toward memory performance was larger than disease duration (based on regression coefficients). For theta, model comparisons in the left Cun ROI indicated that the fit greatly improved with GM volumes (chi = 7.8, p = .005), which was further improved by adding disease duration. The effects of theta on memory scores were significant (left TPJ: b = −4.6, p = .049; left Cun: b = −9.7, p = .025) after controlling for covariates in both ROIs. GM volume tended to be significant in left TPJ (b = 7.3, p = .090), while disease duration was significant in left Cun (b = −0.3, p = .022). The effects of beta on memory scores after controlling for the covariates tended to be significant in the left insula/TPJ (b = 3.3, p = .086) and were no longer significant in left SPL/PreCun. The effects in the left SPL were driven by disease duration (b = −0.3, p = .027). GM volume (b = 5.6, p = .039) and disease duration (b = −0.19, p = .019) along with beta (b = 6.1, p = .018) were significant in the right PCC. Mediation analysis for theta in the left TPJ (b = −2.6, p = .026) and beta in the right PCC (b = 4.3, p = .020) indicated that GM volumes partially mediated the effects of spectral power on memory, whereas no such effects were found for any of the other ROIs. The relationship with alpha was not examined as none of the areas survived the BSR threshold in the whole-brain analysis. Overall, these results suggest that more delta and longer disease duration independently predict severity of memory deficits in PPA, whereas the effects of lesser beta and more theta appear to be partially mediated by GM volumes in some but not all regions.

3.5.3 | PPA RC3-executive function

GM volumes did not improve the model fit in any of the ROIs. After controlling for disease duration, age and GM volumes, alpha (left SFG: b = −30.0, p = .008; right SFG: b = −30.3, p = .016) and theta (right PCC: b = −19.4, p = .041; left SFG: b = −21.4, p = .048; right SFG: b = −25.9, p = .047) significantly predicted EF scores (Supporting Information Table S3). None of the covariates were significant. GM volumes did not improve the model fit in beta ROIs. The effects of beta on EF scores (bilateral PreCun: b = 19.4, p = .006; right lingual: b = 17.9, p = .027; left IFG: b = 14.2, p = .017; left lingual: b = 17.9, p = .010) were significant after controlling for the covariates. The relationship with delta was not examined as none of the areas survived the BSR threshold in the whole-brain analysis. These results indicate that spectral abnormalities across all frequency bands, except delta, predict the severity in EF deficits with minimal to no contribution from GM volumes.

3.5.4 | MCI RC2-memory

The effects of delta on memory scores tended toward significance in the left PreCun (b = −45.0; p = .053), and were significant in the other two ROIs (right PrCG: b = −31.1; p = .049; left Cun: b = −22.3, p = .022), after controlling for age and GM volumes (Supporting Information Table S4). The effects of alpha on memory scores were significant or had a tendency (left lingual: b = 24.3, p = .002; left SFG/MFG: b = 32.9, p = .039; right STG: b = 16.1, p = .063), after controlling for the covariates. The effects of theta on memory scores were not significant in the left paracentral lobe (b = −31.2, p = .14), after controlling for age and GM volumes. Beta was not examined as none of the areas survived the BSR threshold of 4.0. There was no evidence of GM volumes mediating the effects of spectral power on memory scores in any of the frequency bands. Overall, these result patterns suggest that spectral abnormalities in the form of increased delta and reduced alpha uniquely contribute toward memory deficits, more so than volumetric reductions, in MCI.

4 | DISCUSSION

Abnormal spontaneous oscillatory activity may precede frank structural atrophy in dementia due to neuronal and synaptic dysfunction, rather than neuronal death. Cognitive abilities during such intermediate disease stages may be compromised. Therefore, the severity of cognitive deficits may be linked to the degree of abnormal oscillatory activity, reflecting dysfunction, which could help localize specific brain regions that may be more amenable to interventions. While numerous electrophysiological studies have found pathological oscillatory activity in dementia, their relationships with ensuing cognitive impairments and pathology-related structural alterations are less understood. In the present study, we evaluated relationships among specific cognitive deficits, regional volumetric changes, and resting-state MEG (rsMEG) abnormalities in PPA and MCI patients.

Our results indicated the following: (1) Both language and EF abilities were impaired in PPA, whereas episodic memory was impaired in MCI compared with older controls; (2) Despite significant GM shrinkage in both controls and PPA, the pathological findings related to the rsMEG activity in PPA were in stark contrast to those observed in normal aging. While normal aging was linked with widespread oscillatory speeding and GM shrinkage, PPA patients exhibited widespread oscillatory slowing with additional volumetric reductions, encompassing the left-hemispheric language processing areas. Differences in delta and alpha power uniquely predicted group classification to PPA

(vs. controls), with no mediating/indirect effects of GM volumes; (3) The severity of memory and EF deficits in PPA was associated with more delta/theta/alpha, less beta, and smaller GM volumes in specific brain regions but no such relationships were found with language deficits. Lower delta and shorter disease duration, but not GM volumes, uniquely predicted better memory performance. Spectral power across alpha, theta, and beta bands predicted EF abilities with minimal to no contribution from GM reductions. Together, these results suggest that rsMEG activity may emerge from incipient neuronal dysfunction, and not frank atrophy. Electrophysiological dysfunction can be localized to specific brain regions in association with the severity of secondary deficits in PPA such as memory and EF; (4) No evidence for a consistent group difference between MCI and matched controls was found in rsMEG measures. More delta/theta, lesser alpha power, and smaller GM volumes in specific brain regions were related to poorer memory performance. GM volumetric changes associated with memory abilities appeared to be much more widespread than in PPA. The contributions of delta and alpha power, but not theta, on memory abilities were larger than those of GM volume, suggesting that the emergence of this abnormal rsMEG activity may indicate early neuronal dysfunction in the face of ongoing structural changes in MCI.

4.1 | Underpinnings of GM shrinkage and spectral speeding in healthy aging

Numerous prior studies have reported profound structural degradation over a healthy aging trajectory. These changes are thought to be responsible for age-related impairments in cognition, particularly related to worsening processing speed, memory, and EF. Underpinnings of age-related structural changes are typically associated with alterations in the synaptic properties of otherwise intact neurons and neuronal circuits; in contrast the predominant changes in pathological aging as in dementia are related to neuronal death (Fjell & Walhovd, 2010; Morrison & Hof, 2007). Evidence suggests that the inability to maintain high metabolic demands of large neurons, and profound alterations in synaptic plasticity and in gene expression mediate these changes over healthy aging (Fjell & Walhovd, 2010; Konar, Singh, & Thakur, 2016).

While there appears to be a consensus on age-related structural deterioration and its association with cognitive decline, the findings related to oscillatory brain activity, particularly low-frequency power changes, are less consistent (Vlahou, Thurm, Kolassa, & Schlee, 2014). There are reports suggesting either increases (Rossini et al., 2007) or decreases in delta/theta power with increasing age, both of which have been found to be associated with cognitive impairments (Finnigan & Robertson, 2011; Stomrud et al., 2010). Non-linear relationships with age have also been suggested, indicating reversal of delta power from decreases to increases in later life (Gomez et al., 2013; Hashemi et al., 2016). Typically such alterations are accompanied by complementary changes in high-frequency power (alpha/beta) describing the overall shift in toward either slowing or speeding with age. Our analyses comparing older versus younger controls yielded results supporting age-related spectral speeding, however, among older controls we found marginally significant evidence for spectral slowing, lending some support for a nonlinear/U-shaped relationship with age. Spectral speeding in healthy aging could reflect a compensatory mechanism in the wake of diminished nerve conduction velocities (Hong & Rebec, 2012), white matter loss and volumetric changes.

4.2 | Potential mechanisms of volumetric reductions and pathologic spectral slowing in PPA

As noted earlier, we found some evidence for spectral slowing with advanced age among our older controls; however, slowing was amplified in the PPA group and it was accompanied by additional volumetric loss in the left-hemispheric language areas, consistent with prior regional pathology reports (Gorno-Tempini et al., 2004). Approximately 90% of GM volumes, as estimated from structural MRI, comprise neuronal axon collaterals and dendrites, extracellular space, soma and synapses, and the rest is taken up by different glial cells and blood vasculature (Kassem et al., 2013). The observed volumetric reductions in PPA are likely a consequence of the degradation of several of these neuronal processes over time due to the deposition of abnormal proteins, eventually leading to mass neuronal death and volume loss with disease progression.

We found that pathological increases in delta power uniquely contributed to classification into the PPA group, independent of volumetric and sex differences. One of the potential mechanisms of delta increases may be related to the depletion of cholinergic projections from the basal forebrain to the cortex (Schaeverbeke et al., 2017), although this mechanism is more pertinent to AD pathology and therefore to lvPPA than nfvPPA (Rohrer, Rossor, & Warren, 2012). Pathologic slowing of spectral activity has been reported in other clinical populations as well, for example, Stoffers et al. (2007) found slowing in both demented and non-demented Parkinson's disease patients. Based on evidence from a large number of animal and human studies, they speculated that delta abnormalities in demented Parkinson's patients were most likely rooted in the loss of cortical cholinergic activity because of the more widespread damage to this system (Stoffers et al., 2007). In our prior work in left-hemispheric stroke aphasic patients, we also found significant increases in delta power in the perilesional tissue (Kielar et al., 2016). This tissue, while structurally intact, could have suffered from reduced perfusion over time, resulting in synaptic damage. Together, these studies provide a few potential mechanisms that may drive the increases in delta activity in PPA.

4.3 | Functional relevance of spectral abnormalities in PPA and MCI

Elevated delta power predicted poorer episodic memory and EF in PPA, independent of GM volumetric changes. Longer disease duration also predicted poorer memory function, although to a lesser degree. Notably, the effects of theta and beta power with complementary associations with memory scores, could not be readily separated from those of volumetric changes, and in some ROIs such as the right PCC and the left TPJ, volumetric changes mediated the relationship of beta/theta power with memory performance. This was not the case for delta ROIs, suggesting a different mechanism underlying the emergence of delta. The regions involved in delta and memory correlations

in PPA were consistent with a study by Rohrer et al. (2013), who found that lvPPA patients initially exhibit volumetric reductions in the left posterior cortical areas, especially those surrounding the TPJ. Over time, atrophy spreads to more anterior frontotemporal regions and the right-hemispheric homologs of posterior cortical regions, involving the right PCC/precuneus, the medial temporal and the TPJ areas, with worsening language deficits (Rohrer et al., 2013). Based on the progressive pattern of regional involvement, we speculate that the elevated delta in diffuse anterior and medial frontotemporal areas that we found likely reveals ongoing neuronal dysfunction that with the spread of the disease would likely lead to atrophy and result in a complete loss of function. However, the precise neurobiological underpinnings of delta and the ensuing memory dysfunction in PPA remain to be fully explored.

Similar conclusions can be drawn from the spectral and volumetric correlations with EF abilities in PPA. Spectral associations with EF scores were independent of volumetric changes, suggesting neuronal dysfunction rather than atrophy as the underlying mechanism across all frequency bands, that is, this effect was not limited to delta as we saw with the memory impairments. We speculate that executive dysfunction in these patients may be at its early stages, resulting from incipient damage to the neuronal processes, extending beyond the language areas. This is also evident from much more localized associations of volumetric changes with EF abilities than those found with memory. Another possibility is that the observed relationship with EF is in fact mediated by language impairments in these patients. Given that EF tests that loaded on to RC3-EF factor scores had both verbal and nonverbal aspects, it is difficult to distinguish EF from language impairments. There is some evidence suggesting that patients with nfvPPA are comparable to healthy controls in nonverbal cognitive flexibility but are impaired on executive measures mediated by verbal functions (Harciarek & Cosentino, 2013). This would suggest that EF disabilities could emerge as a function of verbal/language deficits in PPA but this notion remains to be explored further.

Echoing some of the findings in PPA, memory decline in MCI was associated with widespread volumetric reductions and spectral slowing, and the effects of volumetric changes in MCI could not be readily separated from those of theta activity. Unlike PPA, however, no evidence of mediation effects of volumetric changes was found for this frequency band. In contrast, delta and alpha contributed relatively more in explaining the memory deficits than GM volumes. This suggests that delta/alpha activity in MCI may reflect neuronal dysfunction, the degree of which reflects the severity of memory deficits. The depletion of cortical cholinergic activity may be responsible for pathologic delta increases affecting the memory function (Schmitz, Nathan Spreng, & Alzheimer's Disease Neuroimaging, 2016). However, the neurobiological underpinnings remain to be fully explored.

Because of the relatively small sample sizes of our patient groups, we express caution against generalization of our findings and recommend substantiation in larger samples in the future. Nonetheless, the combination of participants with two forms of dementia along with both younger and age-matched controls, undergoing a common battery of assessments, provided a unique opportunity in this study to distinguish the structural and electrophysiological changes associated with healthy vs. pathological aging.

5 | CONCLUSIONS AND FUTURE DIRECTIONS

Our findings underscore that rsMEG abnormalities in the form of delta in both PPA and MCI can be used to detect specific brain regions or neuronal populations that may be underperforming and/or at a higher risk of damage. These regions provide targets for interventions such as noninvasive brain stimulation either to normalize the activity or to delay the neurodegenerative process in these regions. However, the onset of such abnormalities, that is, the precise timing of the departure from the normal aging trajectory to a trajectory with accelerated neurodegeneration is largely unknown. Longitudinal assessments of rsMEG activity, starting from preclinical stages to intermediate and fully-developed dementia stages, will address these important knowledge gaps. Additionally, neurobiological processes underlying abnormal oscillatory activity are not well understood and should be explored further. Gaining this knowledge will pave the way for the application of spontaneous oscillatory activity as a neural marker of dementia severity suitable for evaluating the effectiveness of therapeutic interventions.

ACKNOWLEDGMENTS

Funding from the Alzheimer's Association, the Canadian Partnership for Stroke Recovery, the Ontario Brain Institute, and the Canada Research Chairs program. We thank the participating patients, volunteers, and their families.

ORCID

Priyanka P. Shah-Basak https://orcid.org/0000-0003-0763-7381

REFERENCES

Adlam, A. L., Patterson, K., Bozeat, S., & Hodges, J. R. (2010). The Cambridge semantic memory test battery: Detection of semantic deficits in semantic dementia and Alzheimer's disease. *Neurocase*, *16*(3), 193–207. https://doi.org/10.1080/13554790903405693

Ashburner, J. (2007). A fast diffeomorphic image registration algorithm. *NeuroImage*, *38*(1), 95–113. https://doi.org/10.1016/j.neuroimage.2007.07.007

Ashburner, J., & Friston, K. J. (2005). Unified segmentation. *NeuroImage*, *26*(3), 839–851. https://doi.org/10.1016/j.neuroimage.2005.02.018

Benton, A., Hamsher, L., Varney, N. R., & Spreen, O. (1983). *Contributions to neuropsychological assessment: A clinical manual*. New York, NY: Oxford University Press.

Cheyne, D., Bostan, A. C., Gaetz, W., & Pang, E. W. (2007). Event-related beamforming: A robust method for presurgical functional mapping using MEG. *Clinical Neurophysiology*, *118*(8), 1691–1704. https://doi.org/10.1016/j.clinph.2007.05.064

Cho-Reyes, S., & Thompson, C. K. (2012). Verb and sentence production and comprehension in aphasia: Northwestern assessment of verbs and sentences (NAVS). *Aphasiology*, *26*(10), 1250–1277. https://doi.org/10.1080/02687038.2012.693584

Chu, R. K., Braun, A. R., & Meltzer, J. A. (2015). MEG-based detection and localization of perilesional dysfunction in chronic stroke. *Neuroimage: Clinical*, *8*, 157–169. https://doi.org/10.1016/j.nicl.2015.03.019

Delis, D. C., Kaplan, E., & Kramer, J. H. (2001). *Delis-Kaplan the executive function system (D-KEFS)*. San Antonio, TX: The Psychological Corporation.

Dunn, M., & Dunn, L. (1997). *Peabody picture vocabulary test*. Circles Pines, MN: AGS.

Ewers, M., Walsh, C., Trojanowski, J. Q., Shaw, L. M., Petersen, R. C., Jack, C. R., Jr., … North American Alzheimer's Disease Neuroimaging, I. (2012). Prediction of conversion from mild cognitive impairment to Alzheimer's disease dementia based upon biomarkers and neuropsychological test performance. *Neurobiology of Aging*, *33*(7), 1203–1214. https://doi.org/10.1016/j.neurobiolaging.2010.10.019

Fernandez, A., Turrero, A., Zuluaga, P., Gil-Gregorio, P., del Pozo, F., Maestu, F., & Moratti, S. (2013). MEG delta mapping along the healthy aging-Alzheimer's disease continuum: Diagnostic implications. *Journal of Alzheimer's Disease*, *35*(3), 495–507. https://doi.org/10.3233/JAD-121912

Finnigan, S., & Robertson, I. H. (2011). Resting EEG theta power correlates with cognitive performance in healthy older adults. *Psychophysiology*, *48*(8), 1083–1087. https://doi.org/10.1111/j.1469-8986.2010.01173.x

Fjell, A. M., & Walhovd, K. B. (2010). Structural brain changes in aging: Courses, causes and cognitive consequences. *Reviews in the Neurosciences*, *21*(3), 187–221.

Gathercole, S. E., Willis, C. S., Baddeley, A. D., & Emslie, H. (1994). The Children's test of nonword repetition: A test of phonological working memory. *Memory*, *2*(2), 103–127. https://doi.org/10.1080/09658219408258940

Gomez, C., Perez-Macias, J. M., Poza, J., Fernandez, A., & Hornero, R. (2013). Spectral changes in spontaneous MEG activity across the lifespan. *Journal of Neural Engineering*, *10*(6), 066006. https://doi.org/10.1088/1741-2560/10/6/066006

Gorno-Tempini, M. L., Dronkers, N. F., Rankin, K. P., Ogar, J. M., Phengrasamy, L., Rosen, H. J., … Miller, B. L. (2004). Cognition and anatomy in three variants of primary progressive aphasia. *Annals of Neurology*, *55*(3), 335–346. https://doi.org/10.1002/ana.10825

Gorno-Tempini, M. L., Hillis, A. E., Weintraub, S., Kertesz, A., Mendez, M., Cappa, S. F., … Grossman, M. (2011). Classification of primary progressive aphasia and its variants. *Neurology*, *76*(11), 1006–1014. https://doi.org/10.1212/WNL.0b013e31821103e6

Harciarek, M., & Cosentino, S. (2013). Language, executive function and social cognition in the diagnosis of frontotemporal dementia syndromes. *International Review of Psychiatry*, *25*(2), 178–196. https://doi.org/10.3109/09540261.2013.763340

Hardy, C. J. D., Agustus, J. L., Marshall, C. R., Clark, C. N., Russell, L. L., Brotherhood, E. V., … Warren, J. D. (2017). Functional neuroanatomy of speech signal decoding in primary progressive aphasias. *Neurobiology of Aging*, *56*, 190–201. https://doi.org/10.1016/j.neurobiolaging.2017.04.026

Hashemi, A., Pino, L. J., Moffat, G., Mathewson, K. J., Aimone, C., Bennett, P. J., … Sekuler, A. B. (2016). Characterizing population EEG dynamics throughout adulthood. *eNeuro*, *3*(6), ENEURO.0275-16. https://doi.org/10.1523/ENEURO.0275-16.2016

Holschneider, D. P., & Leuchter, A. F. (1995). Beta activity in aging and dementia. *Brain Topography*, *8*(2), 169–180.

Hong, S. L., & Rebec, G. V. (2012). A new perspective on behavioral inconsistency and neural noise in aging: Compensatory speeding of neural communication. *Frontiers in Aging Neuroscience*, *4*, 27. https://doi.org/10.3389/fnagi.2012.00027

Huang, M. X., Mosher, J. C., & Leahy, R. M. (1999). A sensor-weighted overlapping-sphere head model and exhaustive head model comparison for MEG. *Physics in Medicine and Biology*, *44*(2), 423–440.

Kaiser, H. F. (1958). The varimax criterion for analytic rotation in factor analysis. *Psychometrika*, *23*, 187–200.

Kaplan, E., Goodglass, H., & Weintraub, S. (2001). *Boston naming test*. Philadelphia, PA: Lea & Febiger.

Kassem, M. S., Lagopoulos, J., Stait-Gardner, T., Price, W. S., Chohan, T. W., Arnold, J. C., … Bennett, M. R. (2013). Stress-induced grey matter loss determined by MRI is primarily due to loss of dendrites and their synapses. *Molecular Neurobiology*, *47*(2), 645–661. https://doi.org/10.1007/s12035-012-8365-7

Kay, J., Lesser, R., & Coltheart, M. (1996). Psycholinguistic assessments of language processing in aphasia (PALPA): An introduction. *Aphasiology*, *10*(2), 159–180.

Kertesz, A. (1982). *The Western aphasia battery*. New York, NY: Grune & Stratton.

Kielar, A., Deschamps, T., Chu, R. K., Jokel, R., Khatamian, Y. B., Chen, J. J., & Meltzer, J. A. (2016). Identifying dysfunctional cortex: Dissociable effects of stroke and aging on resting state dynamics in MEG and fMRI. *Frontiers in Aging Neuroscience*, *8*, 40. https://doi.org/10.3389/fnagi.2016.00040

Konar, A., Singh, P., & Thakur, M. K. (2016). Age-associated cognitive decline: Insights into molecular switches and recovery avenues. *Aging and Disease*, *7*(2), 121–129. https://doi.org/10.14336/AD.2015.1004

Kriegeskorte, N., Simmons, W. K., Bellgowan, P. S., & Baker, C. I. (2009). Circular analysis in systems neuroscience: The dangers of double dipping. *Nature Neuroscience*, *12*(5), 535–540. https://doi.org/10.1038/nn.2303

Leach, L., Kaplan, E., Rewilak, D., Richards, B., & Proulx, G. (2000). *The Kaplan–Baycrest neurocognitive assessment (KBNA): TEST manual*. San Antonio, TX: Harcourt Assessment.

Leuchter, A. F., Cook, I. A., Newton, T. F., Dunkin, J., Walter, D. O., Rosenberg-Thompson, S., … Weiner, H. (1993). Regional differences in brain electrical activity in dementia: Use of spectral power and spectral ratio measures. *Electroencephalography and Clinical Neurophysiology*, *87*(6), 385–393.

Lopez, M. E., Cuesta, P., Garces, P., Castellanos, P. N., Aurtenetxe, S., Bajo, R., … Fernandez, A. (2014). MEG spectral analysis in subtypes of mild cognitive impairment. *Age (Dordrecht, Netherlands)*, *36*(3), 9624. https://doi.org/10.1007/s11357-014-9624-5

MacKinnon, D. P., Fairchild, A. J., & Fritz, M. S. (2007). Mediation analysis. *Annual Review of Psychology*, *58*, 593–614. https://doi.org/10.1146/annurev.psych.58.110405.085542

Macwhinney, B., Fromm, D., Forbes, M., & Holland, A. (2011). AphasiaBank: Methods for studying discourse. *Aphasiology*, *25*(11), 1286–1307. https://doi.org/10.1080/02687038.2011.589893

McIntosh, A. R., Bookstein, F. L., Haxby, J. V., & Grady, C. L. (1996). Spatial pattern analysis of functional brain images using partial least squares. *NeuroImage*, *3*(3 Pt 1), 143–157. https://doi.org/10.1006/nimg.1996.0016

McIntosh, A. R., & Lobaugh, N. J. (2004). Partial least squares analysis of neuroimaging data: Applications and advances. *NeuroImage*, *23*(Suppl 1), S250–S263. https://doi.org/10.1016/j.neuroimage.2004.07.020

Misic, B., Dunkley, B. T., Sedge, P. A., Da Costa, L., Fatima, Z., Berman, M. G., … Taylor, M. J. (2016). Post-traumatic stress constrains the dynamic repertoire of neural activity. *The Journal of Neuroscience*, *36*(2), 419–431. https://doi.org/10.1523/JNEUROSCI.1506-15.2016

Morrison, J. H., & Hof, P. R. (2007). Life and death of neurons in the aging cerebral cortex. *International Review of Neurobiology*, *81*, 41–57. https://doi.org/10.1016/S0074-7742(06)81004-4

Nasreddine, Z. S., Phillips, N. A., Bedirian, V., Charbonneau, S., Whitehead, V., Collin, I., … Chertkow, H. (2005). The Montreal cognitive assessment, MoCA: A brief screening tool for mild cognitive impairment. *Journal of the American Geriatrics Society*, *53*(4), 695–699. https://doi.org/10.1111/j.1532-5415.2005.53221.x

Petersen, R. C. (2004). Mild cognitive impairment as a diagnostic entity. *Journal of Internal Medicine*, *256*(3), 183–194. https://doi.org/10.1111/j.1365-2796.2004.01388.x

Ranasinghe, K. G., Hinkley, L. B., Beagle, A. J., Mizuiri, D., Honma, S. M., Welch, A. E., … Nagarajan, S. S. (2017). Distinct spatiotemporal patterns of neuronal functional connectivity in primary progressive aphasia variants. *Brain*, *140*(10), 2737–2751. https://doi.org/10.1093/brain/awx217

Rohrer, J. D., Caso, F., Mahoney, C., Henry, M., Rosen, H. J., Rabinovici, G., … Gorno-Tempini, M. L. (2013). Patterns of longitudinal brain atrophy in the logopenic variant of primary progressive aphasia. *Brain and Language*, *127*(2), 121–126. https://doi.org/10.1016/j.bandl.2012.12.008

Rohrer, J. D., Rossor, M. N., & Warren, J. D. (2012). Alzheimer's pathology in primary progressive aphasia. *Neurobiology of Aging*, *33*(4), 744–752. https://doi.org/10.1016/j.neurobiolaging.2010.05.020

Rossini, P. M., Rossi, S., Babiloni, C., & Polich, J. (2007). Clinical neurophysiology of aging brain: From normal aging to neurodegeneration. *Progress in Neurobiology*, *83*(6), 375–400. https://doi.org/10.1016/j.pneurobio.2007.07.010

Schaeverbeke, J., Evenepoel, C., Bruffaerts, R., Van Laere, K., Bormans, G., Dries, E., … Vandenberghe, R. (2017). Cholinergic depletion and basal forebrain volume in primary progressive aphasia. *Neuroimage: Clinical*, *13*, 271–279. https://doi.org/10.1016/j.nicl.2016.11.027

Schmitz, T. W., Nathan Spreng, R., & Alzheimer's Disease Neuroimaging Imaging. (2016). Basal forebrain degeneration precedes and predicts

the cortical spread of Alzheimer's pathology. *Nature Communications*, *7*, 13249. https://doi.org/10.1038/ncomms13249

Smith, C. D., Andersen, A. H., Gold, B. T., & Alzheimer's Disease Neuroimaging Imaging. (2012). Structural brain alterations before mild cognitive impairment in ADNI: Validation of volume loss in a predefined anterotemporal region. *Journal of Alzheimer's Disease*, *31*(Suppl 3), S49–S58. https://doi.org/10.3233/JAD-2012-120157

Sonty, S. P., Mesulam, M. M., Thompson, C. K., Johnson, N. A., Weintraub, S., Parrish, T. B., & Gitelman, D. R. (2003). Primary progressive aphasia: PPA and the language network. *Annals of Neurology*, *53*(1), 35–49. https://doi.org/10.1002/ana.10390

Sonty, S. P., Mesulam, M. M., Weintraub, S., Johnson, N. A., Parrish, T. B., & Gitelman, D. R. (2007). Altered effective connectivity within the language network in primary progressive aphasia. *The Journal of Neuroscience*, *27*(6), 1334–1345. https://doi.org/10.1523/JNEUROSCI.4127-06.2007

Sorg, C., Riedl, V., Muhlau, M., Calhoun, V. D., Eichele, T., Laer, L., … Wohlschlager, A. M. (2007). Selective changes of resting-state networks in individuals at risk for Alzheimer's disease. *Proceedings of the National Academy of Sciences of the United States of America*, *104*(47), 18760–18765. https://doi.org/10.1073/pnas.0708803104

Stoffers, D., Bosboom, J. L., Deijen, J. B., Wolters, E. C., Berendse, H. W., & Stam, C. J. (2007). Slowing of oscillatory brain activity is a stable characteristic of Parkinson's disease without dementia. *Brain*, *130*(Pt 7), 1847–1860. https://doi.org/10.1093/brain/awm034

Stomrud, E., Hansson, O., Minthon, L., Blennow, K., Rosen, I., & Londos, E. (2010). Slowing of EEG correlates with CSF biomarkers and reduced cognitive speed in elderly with normal cognition over 4 years. *Neurobiology of Aging*, *31*(2), 215–223. https://doi.org/10.1016/j.neurobiolaging.2008.03.025

Thomson, D. J. (1982). Spectrum estimation and harmonic analysis. *Proceedings of the IEEE*, *90*(9), 1055–1096.

Tsai, R. M., & Boxer, A. L. (2016). Therapy and clinical trials in frontotemporal dementia: Past, present, and future. *Journal of Neurochemistry*, *138*(Suppl 1), 211–221. https://doi.org/10.1111/jnc.13640

Vlahou, E. L., Thurm, F., Kolassa, I. T., & Schlee, W. (2014). Resting-state slow wave power, healthy aging and cognitive performance. *Scientific Reports*, *4*, 5101. https://doi.org/10.1038/srep05101

Vrba, J. (2002). Magnetoencephalography: The art of finding a needle in a haystack. *Physica C*, *368*, 1–9.

Vrba, J., & Robinson, S. E. (2001). Signal processing in magnetoencephalography. *Methods*, *25*(2), 249–271. https://doi.org/10.1006/meth.2001.1238

Wang, L., Zang, Y., He, Y., Liang, M., Zhang, X., Tian, L., … Li, K. (2006). Changes in hippocampal connectivity in the early stages of Alzheimer's disease: Evidence from resting state fMRI. *NeuroImage*, *31*(2), 496–504. https://doi.org/10.1016/j.neuroimage.2005.12.033

Warrington, E. K. (1984). *Recognition memory test*. Windsor, UK: Nfer-Nelson.

SUPPORTING INFORMATION

Additional supporting information may be found online in the Supporting Information section at the end of the article.

How to cite this article: Shah-Basak PP, Kielar A, Deschamps T, Verhoeff NP, Jokel R, Meltzer J. Spontaneous oscillatory markers of cognitive status in two forms of dementia. *Hum Brain Mapp*. 2019;40:1594–1607. https://doi.org/10.1002/hbm.24470